ChemComm

COMMUNICATION

View Article Online
View Journal | View Issue

Cite this: *Chem. Commun.*, 2025, **61**, 18886

Received 18th September 2025,
Accepted 28th October 2025

DOI: 10.1039/d5cc05378a

rsc.li/chemcomm

Asymmetric kinetic resolution polymerization of racemic *O*-carboxyanhydride catalyzed by cinchona alkaloids

Yanju Jia,[abc] Rulin Yang,*[bcd] Hongguang Sun,*[a] Xuanhua Guo,[bcd] Guangqiang Xu*[bcd] and Qinggang Wang*[bcd]

The enantioselective ring-opening polymerization of *O*-carboxyanhydride (OCA) has been demonstrated for the first time. Utilizing a cinchona alkaloid derivative featuring a confined chiral pocket, the asymmetric kinetic resolution polymerization (AKRP) of racemic OCA was achieved with a kinetic resolution coefficient (k_{rel}) up to 9.0, expanding the application scope of AKRP.

Stereoselective polymerization of monomers with chiral centers is a crucial approach for controlling the micro-stereosequence structure of polymers.[1] It has been extensively studied in the ring-opening polymerization (ROP) of racemic monomers such as epoxides, lactide, and cyclic diolides, *etc.*[2] These processes primarily follow two mechanisms (Scheme 1A): chain-end control (CEC) and enantiomorphic-site control (ESC).[3] Under CEC, the chirality of the chain end determines the chirality of the next monomer to be incorporated. When the preferred chirality of the incoming monomer matches that of the chain end, isoselective stereoblock polymers tend to form, whereas syndiotactic polymers are favored when the chiralities are opposite (Scheme 1A(a)).[4] In the ESC mechanism, the catalyst preferentially recognizes and polymerizes monomers of a specific chirality, a process also referred to as asymmetric kinetic resolution polymerization (AKRP). Depending on the degree of chiral discrimination, isotactic or stereogradient polymers can be obtained (Scheme 1A(b)).[5] In the above catalytic processes, the structure of the catalyst plays a decisive role. Therefore, developing catalytic systems for highly stereoselective polymerization remains a significant demand in AKRP.

Among various chiral monomers, *O*-carboxyanhydrides (OCAs) represent a class of important cyclic monomers worthy of special attention. OCAs can be directly synthesized from α-hydroxy acids or amino acids, making their sourcing environmentally friendly.[6] The variety of monomeric substituents also endows diverse side-chain structures to polymers. Researchers have developed multiple efficient catalytic systems for the ROP of OCAs, enabling good control over polymer molecular weight, dispersity, topology, and suppression of racemization during the process.[7] However, when it comes to controlling the stereoselectivity in the polymerization of racemic OCAs, current studies have primarily relied on the chain-end control mechanism to produce stereoblock or syndiotactic polyesters (Scheme 1B).[8] For instance, Tong's research group reported a Ni/Zn/Ir photoredox catalytic system, which could catalyze ROP of OCAs with different substituents to obtain highly isotactic stereoblock polyesters.[8a] Wu's group reported Zr or Hf-alkoxides with aminotris(phenolate) ligands enabling syndiotactic-selective polymerization of OCA monomers.[8d] Nevertheless, studies on achieving AKRP of OCAs *via* chiral recognition have not been reported in the literature.

In this study, we aim to achieve the AKRP of racemic OCAs (Scheme 1C). Towards this goal, an OCA monomer with a phenethyl substituent was selected as the model monomer, which can be easily prepared from homophenylalanine. The AKRP of this substituent-modified glycolide has been thoroughly investigated by our group.[9] Here, organocatalysis was considered due to its advantages of being metal-free and environmentally friendly. Hence, cinchona alkaloids and their derivatives have attracted our attention. As an important class of chiral organic base catalysts, they are widely used in asymmetric catalysis.[10] In this work, they were introduced into the study of catalyzing the enantioselective ROP of OCA. The correlation between catalyst structure and enantioselectivity was systematically investigated. Through catalyst optimization, a highly enantioselective ROP for OCA was demonstrated for the first time, further expanding the application scope of AKRP.

[a] *College of Polymer Science and Engineering, Qingdao University of Science and Technology, Qingdao, 266042, China. E-mail: hgsun816@qust.edu.cn*
[b] *Key Laboratory of Photoelectric Conversion and Utilization of Solar Energy, Qingdao Institute of Bioenergy and Bioprocess Technology, Chinese Academy of Sciences, Qingdao, 266101, China. E-mail: yangrl@qibebt.ac.cn, xu_gq@qibebt.ac.cn, wangqg@qibebt.ac.cn*
[c] *Shandong Energy Institute, Qingdao, 266042, China*
[d] *Center of Materials Science and Optoelectronics Engineering, University of Chinese Academy of Sciences, Beijing, 100049, China*

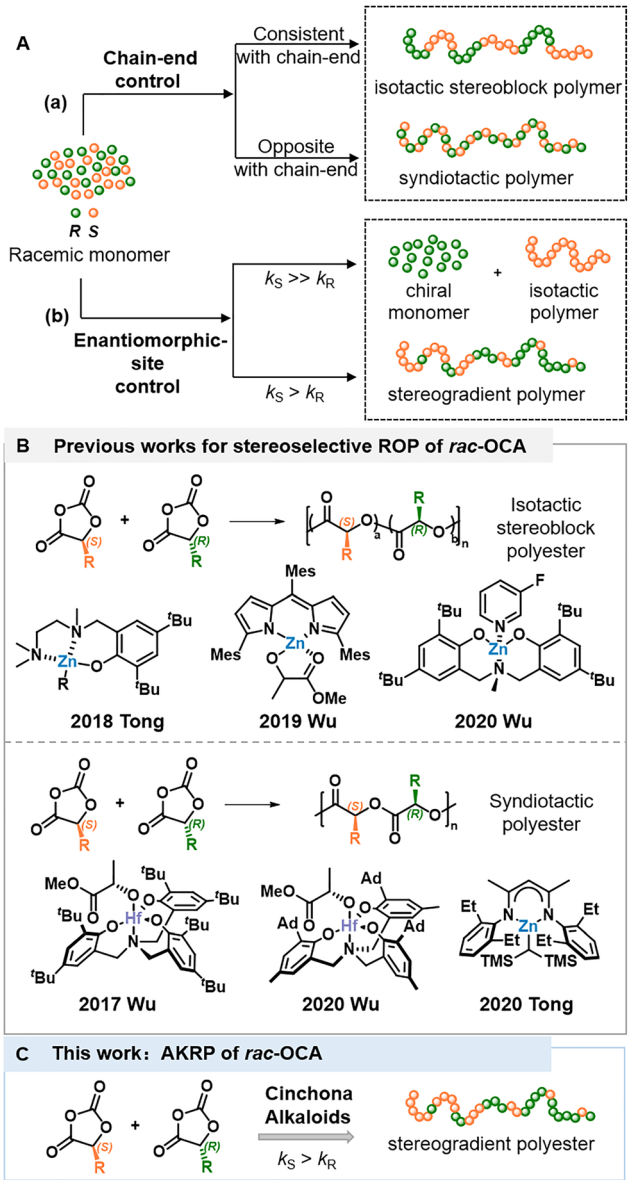

Scheme 1 Stereoselective ROP of *rac*-OCA. (A) Stereoselective control mechanisms. (B) Previous works for stereoselective ROP of *rac*-OCA. (C) AKRP of *rac*-OCA in this work.

Guided by the above research idea, the polymerizations of chiral OCA with two different configurations (*R* and *S*) were first investigated. The reactions were conducted in toluene at room temperature, with an initial ratio of $[Monomer]_0/[Cat.]_0$ = 100/1. The structurally simple, hydroxyl-protected dihydroquinine (Single-*S*, Table 1, entry 1) was initially considered. When it catalyzed the polymerization of *S*-OCA, the reaction reached 97% conversion after 340 min. Kinetic studies indicated that the reaction followed first-order kinetics with a rate constant (k_S) of 0.00917 min^{-1}. In contrast, when *R*-OCA was employed as the monomer, the reaction time extended to 570 min, achieving only 82% conversion, with a rate constant (k_R) of 0.00316 min^{-1}. The calculated rate difference (k_S/k_R) was 2.9-fold (Fig. 1a), suggesting that the cinchona alkaloid Single-*S* possesses chiral recognition towards chirality-matched *S*-OCA.

In our previous research studies, a dual-ligand strategy was proposed to construct a confined chiral space, thereby enhancing the chiral matching between the catalyst and the monomer.[9,11] Inspired by this approach, structural modification of the catalyst through bridged dual-cinchona alkaloids was considered to achieve better chiral recognition towards OCA. Consequently, Dual-*S*-1, featuring an anthraquinone linker structure, was first evaluated (entry 2). However, the rate difference for catalyzing the two chiral OCAs was only 2.8, showing no improvement compared to the single-sided cinchona alkaloid. Further modification involved changing the linker to a diphenylpyrimidine structure (Dual-*S*-2). In this case, *S*-OCA reached 97% conversion in just 70 min, whereas *R*-OCA required an extended reaction time of 360 min to achieve 93% conversion. Analysis of the rate difference obtained an improved value of 6.7 (entry 3), demonstrating the feasibility of optimizing catalyst structure to enhance chiral matching between the catalyst and the monomer.

Encouraged by these results, a linker based on phthalazine (Dual-*S*-3) was further considered (entry 4, Fig. 1b). When catalyzing *S*-OCA, it achieved 98% conversion after 160 min, with a k_S of 0.02217 min^{-1}. For *R*-OCA, there is an induction period in the early stage of the reaction, which may be attributed to the catalyst's inability to effectively activate the mismatched OCA. Then, it reached 96% conversion after a prolonged time of 1410 min, with a k_R of only 0.00225 min^{-1}. Remarkably, a significantly higher rate difference of 9.9-fold was calculated, fully illustrating the excellent enantioselectivity of Dual-*S*-3. The higher chiral recognition of the phthalazine linker suggests that the chiral cavity constructed by this bridged skeleton exhibits stronger chiral matching with the OCA in terms of size, rigidity, and electron distribution. In particular, as previously reported, the nitrogen atoms in the phthalazine linker can interact with the transition state *via* hydrogen bonding, thereby enhancing stereoselectivity.[12]

The research also comparatively examined the influence of catalyst chirality within the skeleton structure. Therefore, Dual-*R*-3, containing a dihydroquinidine unit, was evaluated (entry 5). Experimental results showed that the matched monomer chirality was reversed (entry 4 *vs.* entry 5). The polymerization rate for *R*-OCA was k = 0.01342 min^{-1}, while for *S*-OCA, it was only k = 0.00190 min^{-1}. The calculated rate difference in this case decreased to 7.1. This intriguing outcome indicated that the multiple chiral centers within this catalyst structure act synergistically able to construct a confined chiral space. The opposite configurations of the chiral centers at C8 and C9 of the quinine and quinidine units result in opposite enantioselectivity in catalysis. As diastereomers, their subtle spatial structural differences also lead to variations in the strength of enantioselectivity.

Furthermore, the stereo-discrimination was verified through the polymerization of *rac*-OCA. When catalyzed by Single-*S*, the reaction reached 46% conversion after 285 min (entry 6). Analysis of the enantiomeric excess (*ee*) of the remaining unreacted monomer by chiral high-performance liquid chromatography (HPLC) gave a value of 28.3%. The kinetic

Table 1 ROP of chiral OCA catalyzed by cinchona alkaloids

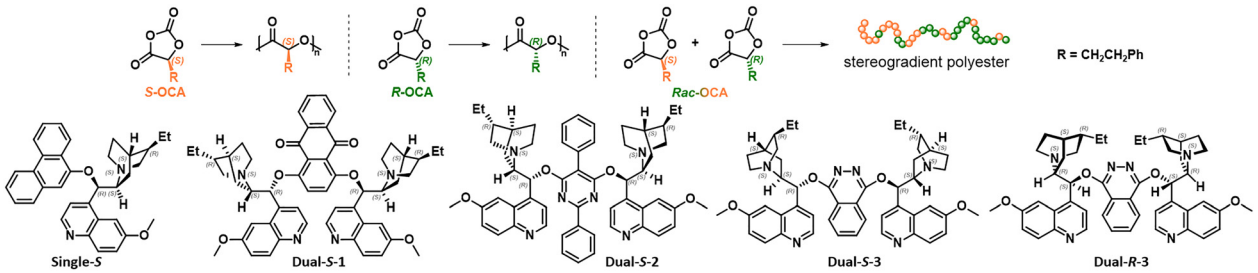

Entry[a]	Cat.	Monomer	Time (min)	Conv.[b] (%)	$M_{n,GPC}$[c] (kDa)	$Đ$[c]	k[d] (min^{-1})	k_{fast}/k_{slow}
1	Single-*S*	*S*	340	97	13.6	1.32	0.00917	2.9
		R	570	82	11.8	1.27	0.00316	
2	Dual-*S*-1	*S*	150	93	11.1	1.41	0.01224	2.8
		R	480	87	7.1	1.35	0.00437	
3	Dual-*S*-2	*S*	70	97	17.4	1.31	0.05543	6.7
		R	360	93	15.3	1.20	0.00823	
4	Dual-*S*-3	*S*	160	98	25.3	1.46	0.02217	9.9
		R	1410	96	14.5	1.23	0.00225	
5	Dual-*R*-3	*S*	1380	91	18.1	1.37	0.00190	7.1
		R	145	82	9.8	1.60	0.01342	
6	Single-*S*	*rac*	285	46	9.2	1.22	—	2.6[e]
7	Dual-*S*-3	*rac*	115	48	11.4	1.28	—	9.0[e]

[a] Conditions: reactions were carried out under a dry nitrogen atmosphere, $[monomer]_0/[cat.]_0$ = 100/1, 0.5 M in toluene, R.T. [b] Determined by ^1H NMR spectra. [c] M_ns and $Đ$s were determined by GPC in THF against polystyrene standards. [d] Rate constant is the slope of the $\ln([M]_0/[M]_t)$ *versus* time relationship graph. [e] For *rac*-OCA, $k_{rel} = \ln[(1 - conv.)/(1 - ee)]/\ln[(1 - conv.)/(1 + ee)]$, with the monomer conversion (conv.) and enantiomeric excess (*ee*) of unreacted monomers.

resolution coefficient (k_{rel}), calculated using the Kagan equation ($k_{rel} = \ln[(1 - conv.)/(1 - ee)]/\ln[(1 - conv.)/(1 + ee)]$), was determined to be 2.6. This result aligns with the earlier conclusion that Single-*S* exhibited chiral recognition towards *S*-OCA. Due to this relatively low stereoselectivity, the reaction kinetics still adhered to a well-defined first-order kinetic model (Fig. 1c). Analysis of the k_{rel} at different conversion revealed a slight increase at the initial stage of the reaction, which subsequently stabilized around 2.5 (Fig. 1d). In contrast, when Dual-*S*-3 was employed, the reaction kinetics revealed a distinct

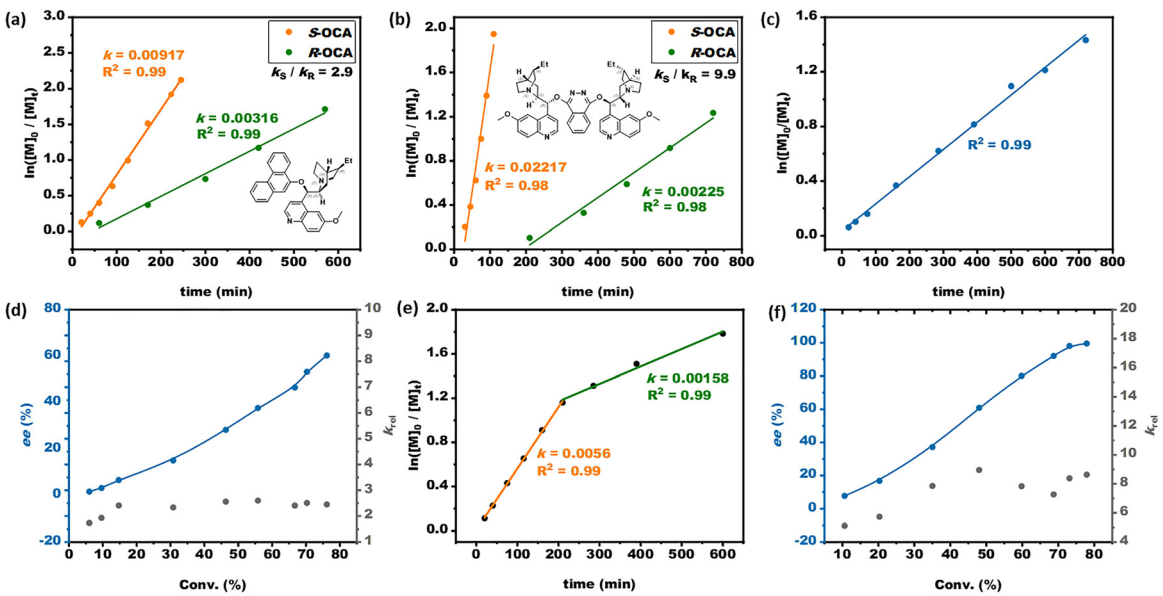

Fig. 1 (a) Kinetic study for Single-*S* catalyzed the ROP of *R*/*S*-OCA. (b) Kinetic study for Dual-*S*-3 catalyzed the ROP of *R*/*S*-OCA. (c) Kinetic study for Single-*S* catalyzed the ROP of *rac*-OCA. (d) The plot of the *ee* value of the unreacted monomer and k_{rel} *versus* conversion for Single-*S* catalyzed the ROP of *rac*-OCA. (e) Kinetic study for Dual-*S*-3 catalyzed the ROP of *rac*-OCA. (f) The plot of the *ee* value of the unreacted monomer and k_{rel} *versus* conversion for Dual-*S*-3 catalyzed the ROP of *rac*-OCA.

inflection point, characterized by a noticeable decrease in the reaction rate (Fig. 1e). This phenomenon is attributed to the rapid consumption of the preferentially polymerized *S*-OCA enantiomer in the early stages of the reaction. In the later stage, the majority of the matched *S*-OCA had been consumed, and the remaining monomer pool became dominated by the less reactive *R*-OCA, leading to an observed decrease in the overall polymerization rate. The high *ee* value of the remaining unreacted monomer also confirmed the preferential consumption of *S*-OCA (Fig. 1f and Table S7). Furthermore, it can be inferred that the resulting polyester possesses a stereogradient microstructure, evolving from a chain segment predominantly derived from the matched (*S*) enantiomer to one with gradually increasing incorporation of the less matched (*R*) enantiomer. Analysis of stereoregularity demonstrated that, in contrast to the atactic polyester obtained with the Single-*S* catalyst, the Dual-*S*-3 catalyst yields an isotacticity-enriched polymer (Fig. S18), further underscoring the high stereoselectivity of Dual-*S*-3. Besides, analysis of the k_{rel} throughout the reaction revealed a noticeable increasing trend before conversion up to approximately 50% (Fig. 1f). At 115 min, with a conversion of 48%, the calculated k_{rel} reached 9.0 (entry 6). Subsequently, the k_{rel} experienced a slight decline. The observed chiral amplification during the initial phase of the reaction suggests that as the polymerization proceeds and the polymer chain grows, improved chiral matching among the catalyst, monomer, and the growing polymer chain occurs. However, after 50% conversion, the increasing relative concentration of the non-preferred enantiomer (*R*-OCA) leads to a decrease in chiral discrimination. This study provides further evidence for the AKRP achieved by the cinchona alkaloid-based catalyst system.

In summary, the chiral recognition and enantioselective polymerization of a phenethyl-substituted OCA monomer was achieved for the first time using chiral cinchona alkaloid catalysis. Through catalyst structural optimization, a polymerization rate difference of up to 9.9-fold between the two chiral OCA monomers was attained. The asymmetric kinetic resolution polymerization of *rac*-OCA was successfully realized, with a k_{rel} reaching 9.0, leading to the preparation of stereogradient polyester materials. This work inspires further research into the stereoselective polymerization of other chiral OCA monomers, advancing the synthesis of chiral polymeric materials.

We are grateful for financial support from the National Natural Science Foundation of China (22571312) and the Taishan Scholars Program of Shandong Province (tstp20240520).

Conflicts of interest

There are no conflicts to declare.

Data availability

The data supporting this article have been included as part of the supplementary information (SI). Supplementary information is available. See DOI: https://doi.org/10.1039/d5cc05378a.

Notes and references

1 (*a*) J.-J. Tian, R. Li, E. C. Quinn, J. Nam, E. R. Chokkapu, Z. Zhang, L. Zhou, R. R. Gowda and E. Y.-X. Chen, *Nature*, 2025, **643**, 967–974; (*b*) M.-Y. Wang, Y.-M. Tu, Q.-Q. Zeng, K. Li, W. Xiong, Z. Cai and J.-B. Zhu, *Nat. Chem.*, 2025, **17**, 1119–1128; (*c*) J. C. Worch, H. Prydderch, S. Jimaja, P. Bexis, M. L. Becker and A. P. Dove, *Nat. Rev. Chem.*, 2019, **3**, 514–535.
2 (*a*) J. Li, B.-H. Ren, Z.-Q. Wan, S.-Y. Chen, Y. Liu, W.-M. Ren and X.-B. Lu, *J. Am. Chem. Soc.*, 2019, **141**, 8937–8942; (*b*) L. S. Morris, M. I. Childers and G. W. Coates, *Angew. Chem., Int. Ed.*, 2018, **57**, 5731–5734; (*c*) X. Tang, A. H. Westlie, E. M. Watson and E. Y.-X. Chen, *Science*, 2019, **366**, 754–758; (*d*) J. Xian, H. Chen, G. Yao, F. Chen, Z. Chen, H. Cao, L. Cao, X. Pan, Y. Tang and J. Wu, *Angew. Chem., Int. Ed.*, 2024, e202420316; (*e*) J. B. Zhu and E. Y.-X. Chen, *J. Am. Chem. Soc.*, 2015, **137**, 12506–12509.
3 (*a*) G. Li, G. Xu, X. Guo, R. Yang, H. Sun and Q. Wang, *ACS Catal.*, 2024, **14**, 1173–1182; (*b*) X. Xie, Z. Huo, E. Jang and R. Tong, *Commun. Chem.*, 2023, **6**, 202.
4 (*a*) S. Abbina and G. Du, *ACS Macro Lett.*, 2014, **3**, 689–692; (*b*) Y.-L. Duan, Q. Guo, G.-Y. Liu, Z.-Z. Yi, S.-P. Feng and Y. Huang, *Polym. Chem.*, 2022, **13**, 4249–4259.
5 (*a*) G. Li, X. Guo, G. Xu and Q. Wang, *Sci. China: Chem.*, 2024, **68**, 1916–1928; (*b*) G. Xu, Q. Mahmood, C. Lv, R. Yang, L. Zhou and Q. Wang, *Coord. Chem. Rev.*, 2020, **414**, 213296.
6 (*a*) A. L. Chin, X. Wang and R. Tong, *Org. Mater.*, 2021, **3**, 41–50; (*b*) Q. Yin, L. Yin, H. Wang and J. Cheng, *Acc. Chem. Res.*, 2015, **48**, 1777–1787.
7 (*a*) Y. Huang, C. Hu, Y. Zhou, R. Duan, Z. Sun, P. Wan, C. Xiao, X. Pang and X. Chen, *Angew. Chem., Int. Ed.*, 2021, **60**, 9274–9278; (*b*) Z. Huo, X. Xie, N. Mahmud, J. C. Worch and R. Tong, *Angew. Chem., Int. Ed.*, 2025, **64**, e202423973; (*c*) M. Li, Y. Tao, J. Tang, Y. Wang, X. Zhang, Y. Tao and X. Wang, *J. Am. Chem. Soc.*, 2019, **141**, 281–289; (*d*) J. Liang, T. Yin, S. Han and J. Yang, *Polym. Chem.*, 2020, **11**, 6944–6952.
8 (*a*) Q. Feng, L. Yang, Y. Zhong, D. Guo, G. Liu, L. Xie, W. Huang and R. Tong, *Nat. Commun.*, 2018, **9**, 1559; (*b*) Y. Cui, J. Jiang, X. Pan and J. Wu, *Chem. Commun.*, 2019, **55**, 12948–12951; (*c*) J. Jiang, Y. Cui, Y. Lu, B. Zhang, X. Pan and J. Wu, *Macromolecules*, 2020, **53**, 946–955; (*d*) Y. Sun, Z. Jia, C. Chen, Y. Cong, X. Mao and J. Wu, *J. Am. Chem. Soc.*, 2017, **139**, 10723–10732; (*e*) Z. Jia, S. Chen, J. Jiang, X. Mao, X. Pan and J. Wu, *Inorg. Chem.*, 2020, **59**, 10353–10360; (*f*) Y. Zhong, Q. Feng, X. Wang, J. Chen, W. Cai and R. Tong, *ACS Macro Lett.*, 2020, **9**, 1114–1118.
9 X. Guo, G. Xu, R. Yang and Q. Wang, *J. Am. Chem. Soc.*, 2024, **146**, 9084–9095.
10 (*a*) H. Becker and K. B. Sharpless, *Angew. Chem., Int. Ed.*, 2003, **35**, 448–451; (*b*) G. M. Miyake and E. Y.-X. Chen, *Macromolecules*, 2011, **44**, 4116–4124; (*c*) R. Yousefi, A. Sarkar, K. D. Ashtekar, D. C. Whitehead, T. Kakeshpour, D. Holmes, P. Reed, J. E. Jackson and B. Borhan, *J. Am. Chem. Soc.*, 2020, **142**, 7179–7189.
11 (*a*) X. Guo, H. Ahmed, G. Xu and Q. Wang, *Angew. Chem., Int. Ed.*, 2025, **64**, e202417075; (*b*) R. Yang, W. Wei, G. Xu, X. Guo and Q. Wang, *Angew. Chem., Int. Ed.*, 2025, **64**, e202504819.
12 S. E. Luderer, B. Masoudi, A. Sarkar, C. Grant, A. Jaganathan, J. E. Jackson and B. Borhan, *J. Org. Chem.*, 2024, **89**, 11921–11929.